Int. J. Appl. Ceram. Technol., 5 [3] 258–264 (2008)
DOI:10.1111/j.1744-7402.2008.02234.x

International Journal of Applied Ceramic Technology
Ceramic Product Development and Commercialization

Net Shape Manufacturing of Three-Dimensional SiCN Ceramic Microstructures Using an Isotropic Shrinkage Method by Introducing Shrinkage Guiders

Tae Woo Lim, Yong Son and Dong-Yol Yang*

Department of Mechanical Engineering, Korea Advanced Institute of Science and Technology, Daejeon 305-701, Korea

Tuan Anh Pham and Dong-Pyo Kim

Department of Fine Chemical Engineering and Chemistry, Chungnam National University, Daejeon 305-764, Korea

Byeong-Il Yang and Kwang-Sup Lee

Department of Advanced Materials, Hannam University, Daejeon 305-811, Korea

Sang Hu Park

School of Mechanical Engineering, Pusan National University, Pusan 609-735, Korea

The two-photon cross-linking (TPC) process using ceramic precursors is recognized as a unique fabrication means of real three-dimensional (3D) ceramic microstructures. These structures can be applied to various microscale devices that are used in harsh conditions that demand high strength, high temperature endurance, and good chemical corrosion properties. However, the large shrinkage amount of 3D structures during pyrolysis is a serious limitation to the practical application of these structures; during pyrolysis, asymmetric distortion and shrinkage occur intrinsically. In an attempt to address this, a method is proposed for the precise fabrication of 3D ceramic microstructures that utilize shrinkage guiders to lead to isotropic shrinkage. SiCN ceramic woodpile structures were fabricated to show the efficiency and usefulness of the proposed method. In the results, the woodpiles showed no distortion after pyrolysis.

Introduction

Polymeric materials have been applied successfully in areas that include ultrasmall scale patterning,

This work was supported by a grant-in-aid for PJT M10503000217-05M0300-21700 by MoST and KOSEF and partially supported by an NCRC program (R15-2006-022-01001-0).
*dyyang@kaist.ac.kr
© 2008 The American Ceramic Society

biochips, optical devices, and many other processes.[1–8] Occasionally, however, these materials do not meet the required properties for use in harsh environments. Devices used in harsh environments must be able to withstand high temperatures and chemical corrosion, and they must have a high mechanical strength. Therefore, the need for novel engineering materials having advantages in terms of their chemical and mechanical properties has significantly increased in the nano/microfabrication field in the fabrication of high value-added nano/micro-devices. The past 10 years has witnessed the rapid progress of three-dimensional (3D) microfabrication using direct laser writing; to date, a variety of 3D applications have been reported that utilize a range of engineering materials, including polymers and metals.[9–12] Moreover, recent research has proposed the direct fabrication of 3D ceramic structures with a high spatial resolution using a polymeric ceramic precursor cross-linked by two-photon absorption (TPA) for 3D shaping and transformed to a SiCN ceramic state by pyrolysis.[13] This process paves the way for the direct fabrication of complex 3D ceramic microstructures with a resolution near 200 nm; it may become increasingly utilized for the fabrication of various innovative ceramic applications in the near future, replacing the conventional processes of mechanical machining, molding, and photolithography.[14–19]

However, a severe shrinkage phenomenon that inevitably occurs during pyrolysis of polymeric ceramic precursors is recognized as the most important issue related to the practical use of this method; particularly, shape distortion accompanied by anisotropic shrinkage is a serious problem that must be resolved before application of these materials to mechanical and photonic devices requiring precise construction, such as microrotors and photonic crystals, can become a reality.[15,16,19–21] It is well known that the pyrolytic transformation from low-density polymers to high-density ceramics intrinsically leads to inevitable volume shrinkage. In a previous work by some of the authors of this work, a mixture of silica (SiO_2) nanoparticles and a precursor was utilized to improve the shrinkage amount. By increasing the volume of silica particles in the precursor, the shrinkage amount was progressively reduced.[13] This was moderately effective, but when the amount of SiO_2 particles was $>50\%$ in the mixture, direct 3D shaping via TPA was not easy because of the muddiness of the mixture; moreover, the surface roughness of the microstructures became much coarser with the increase of the mixture ratio of SiO_2. If a large amount of shrinkage occurred, cracks and considerable residual stress remained inside the structure after pyrolysis. To overcome this problem, this study proposes an isotropic shrinkage method (ISM) that introduces shrinkage guiders.

Experimental Procedures

The fundamental cause for anisotropic shrinkage of a 3D microstructure during a pyrolysis process is a constraint condition related to the attachment of the bottom side of the microstructure to a substrate (glass plate). Therefore, shrinkage guiders are introduced, which control the shrinkage of 3D microstructures in all directions (isotropic shrinkage) in the ISM. Using this method, the fabrication of precise 3D ceramic microstructures without shape distortions is possible even when a very large amount of shrinkage occurs during the pyrolysis process. Figure 1a and b illustrate schematically the difference in terms of the shrinkage mechanism between anisotropic shrinkage and isotropic shrinkage. With isotropic shrinkage (see Fig. 1b), the initial length (d_0) and height (h_0) of a woodpile become d_{f2} and h_{f2} using shrinkage guiders, respectively, without distortion. Otherwise, the final lengths of the top and bottom sides do not shrink at the same rate because of adhesion of the bottom side to the substrate (anisotropic shrinkage): d_0 shrinks to d_{f1} on the top and d_0 to the same d_0 at the bottom. Therefore, in previous works, it was not possible to fabricate ceramic microstructures without distortion.

The shrinkage guiders are designed and fabricated as slender rods having several hundred nanometers width for free bending and free shrinkage without any influence on the main structure. Hence, they may be deformed readily because of the surface tension of a rinsing material in a developing process. To solve this problem and to enhance the mechanical stability of the microstructures in the rinsing process, a photocurable resin with a high strength after photoshaping is required in the ISM. For this reason, functionalized photosensitive polyvinylsilazane as a transparent solid phase with a high molecular weight (HM–PVS) was synthesized via the modification of solid polyvinylsilazane (KiON Ultra Polysilazane, KiON, Charlotte, NC) through linkage and/or insertion reaction routes with the addition of 2-isocyanatoethyl methacrylate (ICEM, Hestia

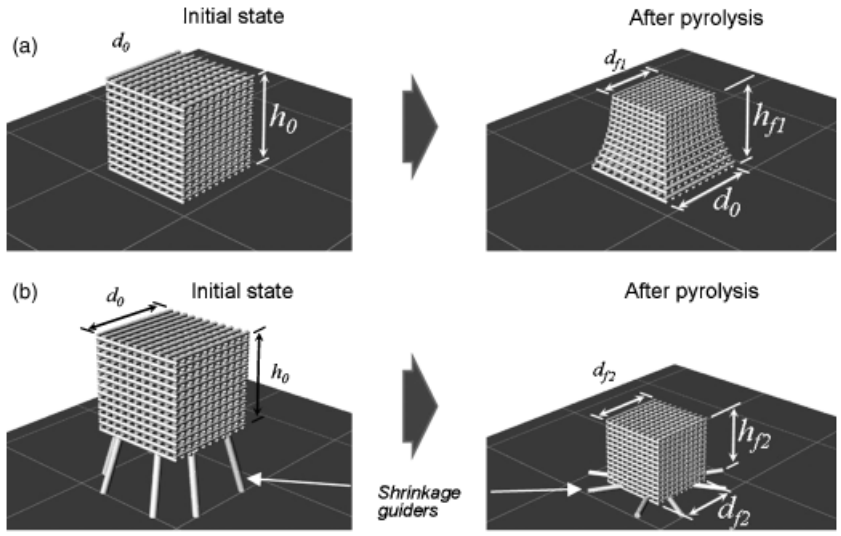

Fig. 1. Processes of (a) anisotropic shrinkage and (b) isotropic shrinkage of woodpile structures. Anisotropic shrinkage occurs because of the bottom surfaces of the structures sticking to the substrates strongly. The body structure, woodpile structure in this figure, can shrink isotropically by using the isotropic shrinkage method by introducing shrinkage guiders.

Laboratories, New Berlin, WI) at a ratio of 20 wt%, following a report published by the authors concerning the synthesis of low-molecular-weight methacrylated polyvinylsilazane (LM–PVS).[13] The molecular weight of HM–PVS increased slightly from 8940 to 10,366, as measured by gel permeation chromatography (GPC), presumably due to the addition of methacrylate groups into the mother polymer (Mn = 8940). According to a nano-indentation test, HM–PVS has an elastic modulus of 4 GPa after cross-linking without the use of a nanoparticle filler. This is four times stronger than that of cured LM–PVS (approximately 1 GPa) (see Fig. 2). The improved strength of the cured HM–PVS obviously provided reliable stability against the mechanical deformation induced by the surface tension of rinsing solvents during the developing process, while the fabricated microstructures from LM–PVS were troublesomely collapsed at this step. Moreover, the HM–PVS resin has 75.5 wt% of ceramic yield at 1000°C, which is a relatively high ceramic yield when a dense ceramic product with less shrinkage is obtained during thermal conversion to the ceramic phase by pyrolysis. To increase the sensitivity in photo-crosslinking, a two-photon absorbing photosensitizer [1,4-bis(2-ethylhexyloxy)-2,5-bis(2-(4-(bis(4-bromophenyl)amino))vinyl)benzene] (EA4-BPA–VB) of 0.4 wt% was mixed into the HM–PVS after dilution in a tetrahydrofuran (THF) solvent.[22]

A drop of the HM–PVS resin solution was placed on a thin glass plate and the solvent was completely removed in a vacuum condition. A nano-stereolithography (NSL) process employing TPA was utilized for the creation of 3D microstructures.[23–26] As illustrated in Fig. 3, 3D two-photon cross-linked structures were created via forward layer-by-layer accumulation with a

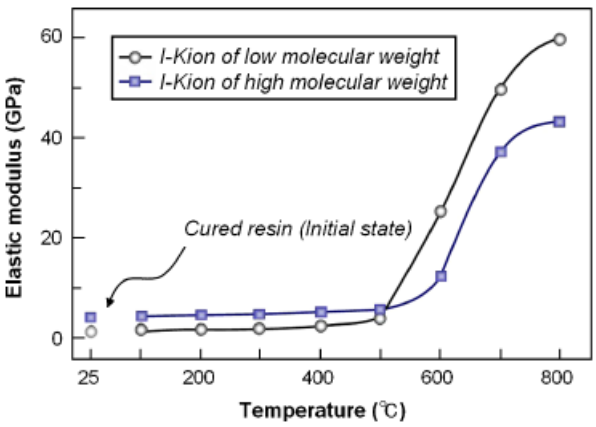

Fig. 2. Dependence of elastic modulus on spin-coated polymer films, UV-cured and pyrolyzed at various temperatures. The polymer films were cured by UV exposure at 20 mW/cm^2 for 10 min and then annealed at various temperatures (100–800°C) in a tube furnace in a nitrogen atmosphere.

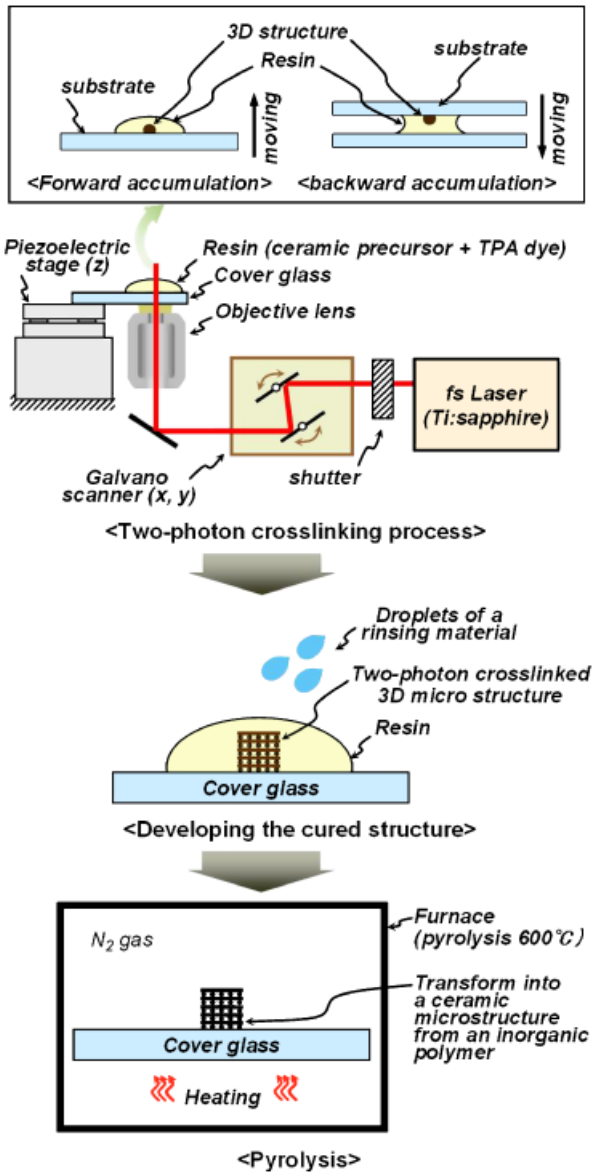

Fig. 3. Complete process of the 3D ceramic microfabrication. The ceramic precursor is shaped by the curing process, two-photon induced nano-stereolithography. The inset illustrates forward accumulation and backward accumulation; the former is simpler and stabler than the latter method. When the change of refractive index is large, the backward accumulation method is required.

submicrometer resolution, which is simpler and stabler than the backward accumulation process. Here, it is worth noting that a change of the refractive index of the resin before and after cross-linking is an important criterion in the selection of a suitable accumulation method. In the case of HM–PVS, the difference of the refractive index was 0.008 from 1.493 to 1.501; therefore, building 3D microstructures using the forward accumulation method was not so complicated with the negligible change of the refractive index. The 3D inorganic microstructures fabricated via NSL can be transformed to 3D ceramic microstructures via pyrolysis. Figure 3 shows a schematic of the procedure for 3D ceramic microstructures.

Results and Discussions

Experimental results of a parameter study of the variation of the line width according to the laser dose (power and exposure time) are shown in Fig. 4a. With a decrease of the laser dose, the line width was progressively reduced. The smallest line width of 180 nm was achieved under a laser power of 30 mW and a duration time of 1 ms. To verify the shrinkage amount explicitly after pyrolysis, a woodpile microstructure without a shrinkage guider was fabricated, as shown in Fig. 4b. Its bottom side was attached strongly to a glass plate and had no dimensional change, but the top side shrank freely from 9 to 5.92 μm; the shrinkage varied anisotropically from the bottom to the top side, and the maximal shrinkage of 33% occurred at the top side after pyrolysis. To solve the problem of shape distortion during pyrolysis, the woodpile was redesigned with shrinkage guiders at its bottom edges (see the initial structure of Fig. 1b). In the ISM, it was assumed that the strength of a 3D microstructure is much higher than that of the thin shrinkage guiders; it was assumed sufficient to bend the guiders without influencing the body structure and leading to isotropic shrinkage. There are a number of design parameters for the shrinkage guiders, including the connecting positions, number of guiders (n), size of the cross-section (s), inclination angle (θ), and the initial length (l_i) of guiders. The connecting positions with a main body structure are determined as a group with the same horizontal displacement (δ) on the bottom contours of the body structures before and after isotropic shrinkage. As n increases, s can be reduced to provide free bending of the guiders only at the edge joint of the body structure; the group with maximal connecting positions (n) is then selected. For the woodpile structure, a group consisting of eight guiders was selected (see Fig. 5a and b). The shrinkage guiders were all 0.5 μm in diameter. To increase the stability for the horizontal forces

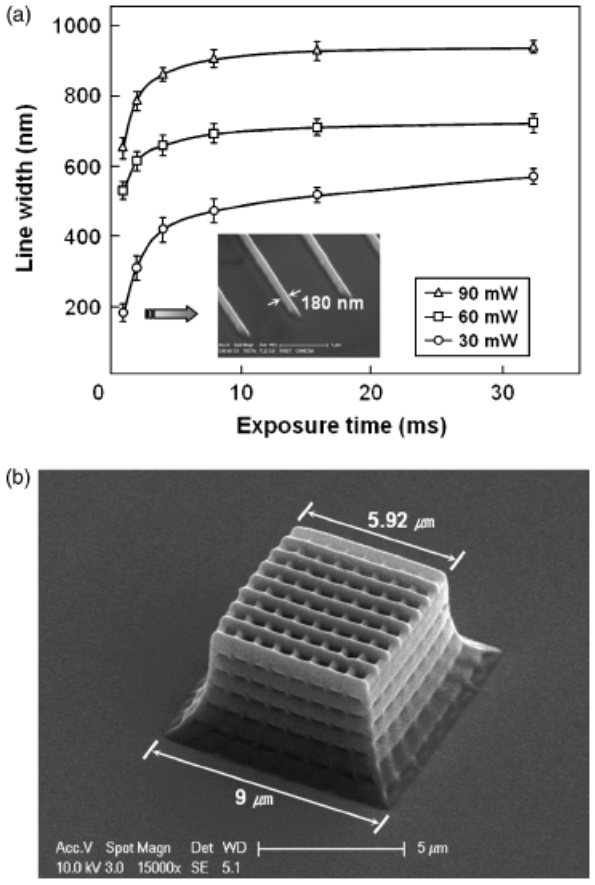

Fig. 4. (a) Dependence of the line width of the polymeric phase on the laser power and the exposure time as processing parameters of the nano-stereolithography. The resolution of this process is about 180 nm, which is smallest in 3D ceramic fabrication processes. (b) When the woodpile microstructure with dimensions of 9 μm × 9 μm × 9 μm was pyrolyzed at 600°C under N_2, the adhered structure to the substrate was anisotropically shrunk to the dimension of 5.92 μm top length and 9 μm bottom length.

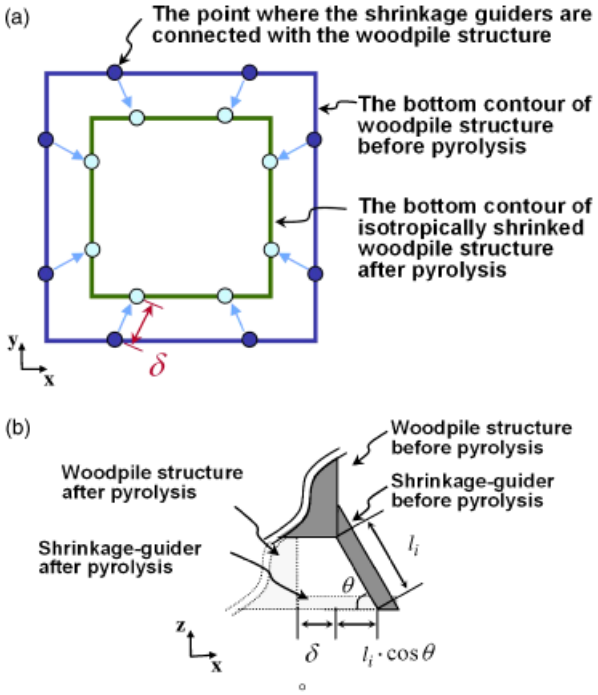

Fig. 5. (a) A bottom contour of the woodpile structure before pyrolysis, a bottom contour of an isotropically shrunk woodpile structure after pyrolysis, and eight pairs of points which are the points connecting with the shrinkage guiders. (b) Schematic diagram of the formations of shrinkage guiders before and after pyrolyis. When the body structure, woodpile structure in this work, sticks to the substrate simultaneously with the end of the pyrolysis, the initial length of the guiders can be calculated from θ, δ, *and* ε.

during the development process, the guiders were designed to incline. In a preliminary test, the woodpile structures with the guiders at an inclination below 75° were developed firmly without collapsing.

During pyrolysis, owing to the free bending of the guiders, the body structures shrink isotropically and gradually approach the substrate. A stable and nondistorted ceramic microstructure can be obtained when the body structure sticks to the substrate simultaneously at the end of pyrolysis, which is the ideal mode of the ISM. From the schematic diagram of the shrinkage guiders before and after pyrolysis shown in Fig. 5b, the initial length (l_i) of the guiders for the ideal mode can be derived as $\delta/(1-\varepsilon-\cos\theta)$, where ε is the shrinkage rate obtained from the preliminary test.

To estimate the effectiveness of the ISM, woodpile structures of a dimension of 9 μm × 9 μm × 9 μm with shrinkage guiders with values of l_i from 1 to 5 μm were fabricated (see Fig. 6a) and pyrolyzed (see Fig. 6b–d). When $\varepsilon = 0.34$, $\delta = 1.72$, and $\theta = 75°$, l_i in the ideal mode is calculated as 4.2 μm. Using this value of l_i, a precise ceramic woodpile structure could be obtained without distortion despite the large amount of shrinkage, as shown in Fig. 6c. When the initial length is shorter than $\delta/(1-\varepsilon-\cos\theta)$, the body structure sticks to the substrate before the entire pyrolysis process is finished; at that time, it experiences anisotropic shrinkage when the subsequent pyrolysis process is finished, as shown in Fig. 6b. As the length becomes longer, the distortion of the structure is improved as shown in

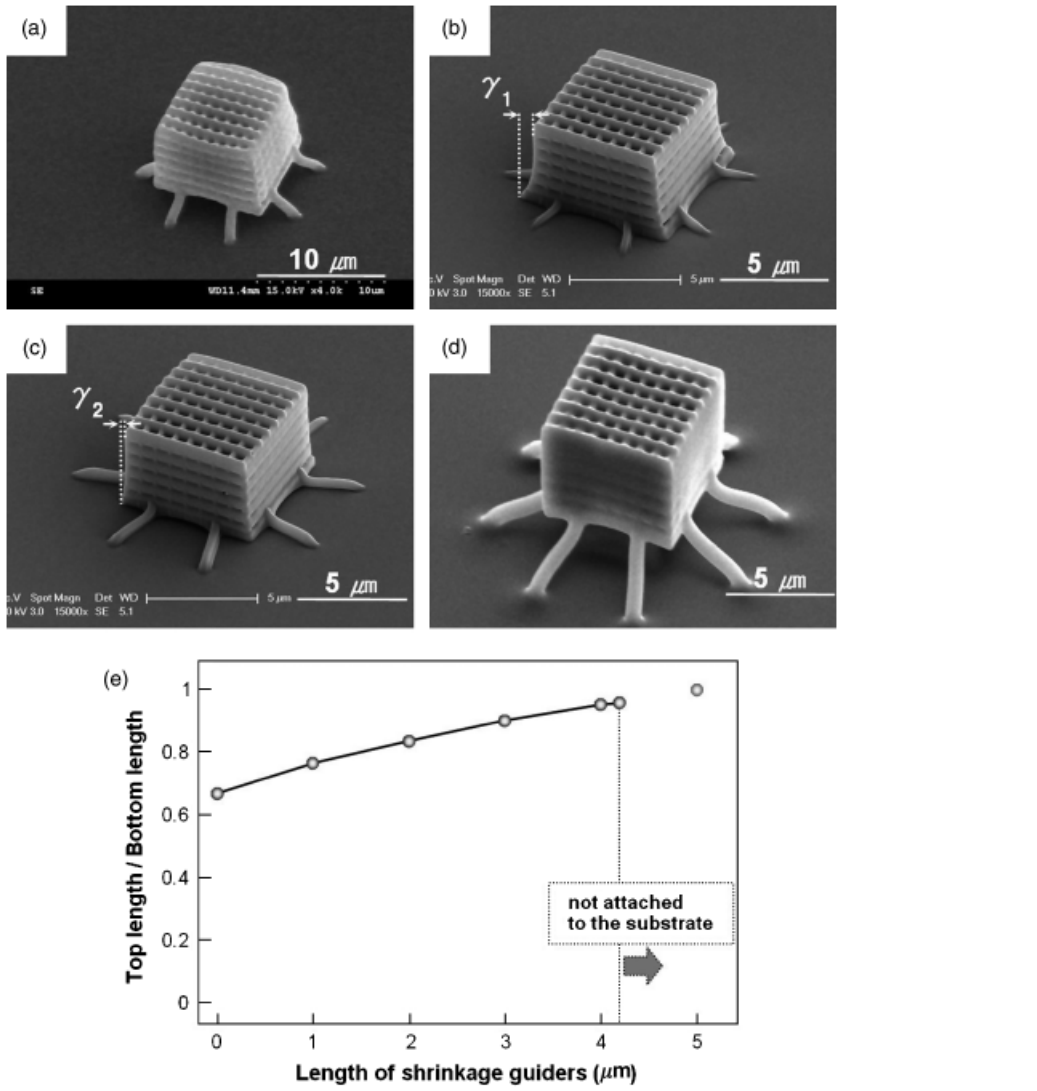

Fig. 6. (a) A two-photon cross-linked woodpile structure with shrinkage guiders, and (b–d) pyrolized ceramic woodpile structures with shrinkage guiders of various lengths (2.0, 4.2, and 6.0 μm, respectively). By increasing the lengths of the guiders, the distortion of the structures is reduced ($\gamma_1 > \gamma_2$). When a ceramic microstructure at some distance from the substrate is required, it can be obtained by designing the length long enough. (e) Top length/bottom length versus length of the guiders.

Fig. 6e. If the length is longer than $\delta/(1-\varepsilon-\cos\theta)$, the body structure remains supported by guiders after the pyrolysis process finishes, as shown in Fig. 6d. However, the distance between the body structure and the substrate can be estimated from the design parameters of the guiders, and this shrinkage mode can be used when structures at some distance from the substrate are required.

Conclusions

In summary, an ISM that uses shrinkage guiders is proposed here to address an issue related to shrinkage, which is recognized as a significant problem in ceramic microfabrication processes using ceramic precursors. Suitable design parameters for the shrinkage guiders can be determined by considering the shrinkage and the

body structures in the ISM. For this method, materials with high strength after photo-crosslinking are required to increase the stability in the development process; a ceramic precursor with a high molecular weight (HM–PVS) was able to satisfy these requirements. According to the fabrication results of woodpile structures utilizing shrinkage guiders, it was possible to confirm that the ISM is an effective method for the fabrication of 3D precise ceramic microstructures that do not experience distortion or residual stress.

References

1. B. H. Cumpston, S. P. Ananthavel, S. Barlow, D. L. Dyer, J. E. Ehrlich, L. L. Erskine, A. A. Heikal, S. M. Kuebler, I.-Y. S. Lee, D. M. Maughon, J. Qin, H. Rockel, M. Rumi, X. L. Wu, S. R. Marder, and J. W. Perry, "Two-Photon Polymerization Initiators for Three-Dimensional Optical Data Storage and Microfabrication," *Nature*, 398 51–54 (1999).
2. S. W. Jeon, J. U. Park, R. Cirelli, S. Yang, C. E. Heitzman, P. V. Braun, P. J. A. Kenis, and J. A. Rogers, "Fabricating Complex Three-Dimensional Nanostructures with High-Resolution Conformable Phase Masks," *Proc. Natl. Acad. Sci.*, 101 [34] 12428–12433 (2004).
3. S. Maruo, K. Ikuta, and H. Korogi, "Submicron Manipulation Tools Driven by Light in a Liquid," *Appl. Phys. Lett.*, 82 [1] 133–135 (2003).
4. L. H. Nguyen, M. Straub, and M. Gu, "Acrylate-Based Photopolymer for Two-Photon Microfabrication and Photonic Applications," *Adv. Funct. Mater.*, 15 [2] 209–216 (2005).
5. M. Sraub and M. Gu, "Near-Infrared Photonic Crystals with Higher-Order Bandgaps Generated by Two-Photon Photopolymerization," *Opt. Lett.*, 27 [20] 1824–1826 (2002).
6. J. L. Yang, S. J. An, W. I. Park, G. C. Yi, and W. Choi, "Photocatalysis Using ZnO Thin Films and Nanoneedles Grown by Metal–Organic Chemical Vapor Deposition," *Adv. Mater.*, 16 [18] 1661–1664 (2004).
7. H. B. Sun, K. Takada, and S. Kawata, "Elastic Force Analysis of Functional Polymer Submicron Oscillators," *Appl. Phys. Lett.*, 79 [19] 3173–3175 (2001).
8. T. Watanabe, M. Akiyama, K. Totani, S. M. Kuebler, F. Stellacci, W. Wenseleers, K. Braun, S. R. Marder, and J. W. Perry, "Photoresponsive Hydrogel Microstructure Fabricated by Two-Photon Initiated Polymerization," *Adv. Funct. Mater.*, 12 [9] 611–614 (2002).
9. F. Stellacci, C. A. Bauer, T. Meyer-Friedrichsen, W. Wenseleers, V. Alain, S. M. Kuebler, S. J. K. Pond, Y. Zhang, S. R. Marder, and J. W. Perry, "Laser and Electron-Beam Induced Growth of Nanoparticles for 2D and 3D Metal Patterning," *Adv. Mater.*, 14 [3] 194–198 (2002).
10. K. Kaneko, H. B. Sun, X. M. Duan, and S. Kawata, "Two-Photon Photoreduction of Metallic Nanoparticle Gratings in a Polymer Matrix," *Appl. Phys. Lett.*, 83 [7] 1426–1428 (2003).
11. N. Tosaa, J. Bossona, M. Pierrea, C. Rambauda, M. Bouriaua, G. Vitrantb, O. Stéphana, S. Astileanc, and P. L. Baldeck, "Optical Properties of Metallic Nanostructures Fabricated by Two-Photon Induced Photoreduction," *Proc. SPIE*, 6195 619501 (2006).
12. C. Sun and X. Zhang, "The Influences of the Material Properties on Ceramic Micro-Stereolithography," *Sensor Actuators A*, 101 364–370 (2002).
13. T. A. Pham, D. P. Kim, T. W. Lim, S. H. Park, D. Y. Yang, and K. S. Lee, "Three-Dimensional SiCN Ceramic Microstructures Via Nano-Stereolithography of Inorganic Polymer Photoresists," *Adv. Funct. Mater.*, 16 [9] 1235–1241 (2006).
14. G. Feiertag, W. Ehrfeld, H. Freimuth, H. Kolle, H. Lehr, M. Schmidt, M. M. Sigalas, C. M. Soukoulis, G. Kiriakidis, T. Pedersen, J. Kuhl, and W. Koenig, "Fabrication of Photonic Crystals by Deep X-Ray Lithography," *Appl. Phys. Lett.*, 71 [11] 1441–1443 (1997).
15. H. Yang, P. Deschatelets, S. T. Brittain, and G. M. Whitesides, "Fabrication of High Performance Ceramic Microstructures from a Polymeric Precursor Using Soft Lithography," *Adv. Mater.*, 13 [1] 54–58 (2001).
16. L. A. Liew, Y. Liu, R. Luo, T. Cross, L. An, V. M. Bright, M. L. Dunn, J. W. Daily, and R. Raj, "Fabrication of SiCN MEMS by Photopolymerization of Pre-Ceramic Polymer," *Sensor Actuators*, 95 120–134 (2002).
17. C. Provin, S. Monneret, H. L. Gall, and S. Corbel, "Three-Dimensional Ceramic Microcomponents Made Using Microstereolithography," *Adv. Mater.*, 15 [12] 994–997 (2003).
18. M. Schulz, M. Börner, J. Haubelt, and R. Heldele, "Polymer Derived Ceramic Microparts from X-Ray Lithography—Cross-Linking Behavior and Process Optimization," *J. Eur. Ceram. Soc.*, 25 199–204 (2005).
19. S. J. Ahn and J. H. Moon, "Vacuum-Assisted Microfluidic Lithography of Ceramic Microstructures," *Int. J. Appl. Ceram. Technol.*, 88 [5] 1171–1174 (2005).
20. S. Passinger, M. S. M. Saifullah, C. Reinhardt, K. R. V. Subramanian, B. N. Chichkov, and M. E. Welland, "Direct 3D Patterning of TiO_2 Using Femtosecond Laser Pulses," *Adv. Mater.*, 19 [9] 1218–1221 (2007).
21. C. A. Lewinsohn, P. Colombo, I. Reimanis, and Ö. Ünal, "Stresses Occuring During Joining of Ceramics Using Preceramic Polymers," *Int. J. Appl. Ceram. Technol.*, 84 [10] 2240–2244 (2001).
22. K. S. Lee, M. S. Kim, H. K. Yang, B. K. So, H. B. Sun, S. Kawata, and P. Fleitz, "Molecular Crystals and Liquid Crystals," *Mol. Cryst. Liq. Cryst.*, 424 35–41 (2004).
23. J. Serbin, A. Egbert, A. Ostendorf, B. N. Chichkov, R. Houbertz, G. Domann, J. Schulz, C. Cronauer, L. Froehlich, and M. Popall, "Femtosecond Laser-Induced Two-Photon Polymerization of Inorganic Organic Hybrid Materials for Applications in Photonics," *Opt. Lett.*, 28 [5] 301–303 (2003).
24. K. K. Seet, V. Mizeikis, S. Matsuo, S. Juodkazis, and H. Misawa, "Three-Dimensional Spiral-Architecture Photonic Crystals Obtained by Direct Laser Writing," *Adv. Mater.*, 17 [5] 541 (2005).
25. C. A. Coenjarts and C. K. Ober, "Two-Photon Three-Dimensional Microfabrication of Polydimethylsiloxane Elastomers," *Chem. Mater.*, 16 5556–5558 (2004).
26. D. Y. Yang, S. H. Park, T. W. Lim, H. J. Kong, S. W. Yi, H. K. Yang, and K. S. Lee, "Ultraprecise Microreproduction of a Three-Dimensional Artistic Sculpture by Multipath Scanning Method in Two-Photon Photopolymerization," *Appl. Phys. Lett.*, 90 [1] 013113 (2007).